

Modelling thermohaline variable-density flow and solute transport in fractured porous media

T. GRAF & R. THERRIEN

*Department of Geology and Geological Engineering, Université Laval, Ste-Foy,
Québec G1K 7P4, Canada*

thomas.graf.1@ulaval.ca

Abstract The discrete-fracture numerical model FRAC3DVS has been enhanced to simulate thermohaline variable-density flow and solute transport in fractured porous media. A general formulation of the buoyancy term has been derived to simulate density effects in irregular networks of discrete fractures with arbitrary incline. The model allows the investigation of variable-density flow in more disorganized fractured media than previously possible. A series of simulations in different, yet statistically equivalent, fracture networks has been conducted and show that solute migration is highly sensitive to the properties of the network. A sensitivity analysis reveals that low fracture apertures, low matrix permeability, high matrix porosity and large molecular diffusion, tend to stabilize solute migration.

Keywords fractured rock; FRAC3DVS; numerical modelling; variable-density flow

INTRODUCTION

Variable-density fluid flow and solute transport is of concern in several areas in geosciences, such as saltwater intrusion and nuclear waste disposal. Detailed studies of dense plume migration have been conducted predominantly in homogeneous and heterogeneous porous media, Fig. 1(a) and (b). However, there are a limited number of studies of density effects in fractured geological formations. Shikaze *et al.* (1998) investigated the migration of dense plumes in discretely-fractured media, using an orthogonal fracture network embedded in a porous matrix, Fig. 1(c). They found that dense solute plumes may develop in a highly irregular fashion and the uncertainty associated with prediction can be very high. However, their simulations only considered orthogonal fracture networks and uniform fracture apertures. Therefore, how dense plume instabilities will develop in fractured networks with an irregular pattern (Fig. 1(d)) remains unknown.

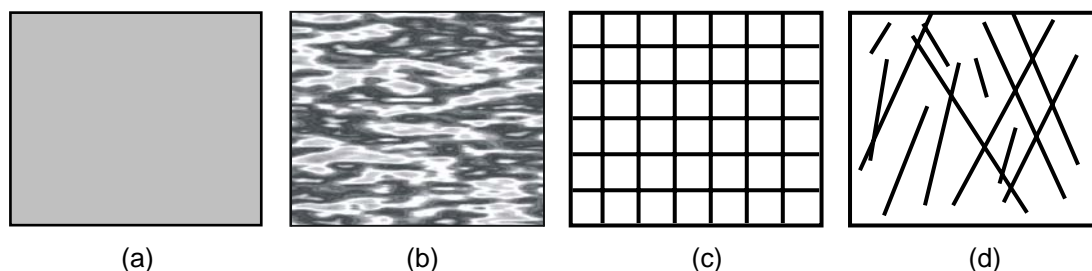


Fig. 1 Different styles of geological media: (a) homogeneous porous medium, (b) heterogeneous porous medium, (c) fractured medium consisting of vertical and horizontal fractures and (d) fractured geological medium with nonuniform fracture aperture, trace and orientation (modified from Simmons *et al.*, 2001).

To address this question, the FRAC3DVS model (Therrien & Sudicky, 1996), which solves three-dimensional (3-D) variably-saturated flow and solute transport in discretely-fractured porous media, has been modified to account for density and viscosity variations in irregular fracture networks. Variations in fluid properties are calculated as functions of both salinity and temperature.

NUMERICAL MODEL

Governing equations

The following three equations describe 3-D thermohaline variable-density flow and solute transport in porous media (Bear, 1988; Holzbecher, 1998):

$$\frac{\partial}{\partial t}\{\phi\rho\} = -\nabla \bullet \{\phi\rho\mathbf{v}\} \pm \Gamma_{mass} \quad (1)$$

$$\frac{\partial}{\partial t}\{\phi C\} = -\nabla \bullet \mathbf{J}_{solute} \pm \Gamma_{solute} \quad (2)$$

$$\frac{\partial}{\partial t}\{(\rho\tilde{c})_b T\} = -\nabla \bullet \mathbf{J}_{heat} \pm \Gamma_{heat} \quad (3)$$

where equations (1), (2), and (3) are for fluid flow, solute transport and heat transfer, respectively. The dimensionless matrix porosity is given by ϕ , while ρ [M L^{-3}] is the fluid density, \mathbf{v} [L T^{-1}] is the average fluid velocity, C [M L^{-3}] is the solute concentration, t [T] is time, ∇ [L^{-1}] is the divergence operator, $(\rho\tilde{c})_b$ [$\text{M L}^{-1} \text{T}^{-2} \text{ } ^\circ\text{C}^{-1}$] is the bulk heat capacity and T [$^\circ\text{C}$] is temperature. The solute mass flux and the thermal energy flux are represented by \mathbf{J}_{solute} and \mathbf{J}_{heat} , respectively, and Γ denotes sources and sinks.

The fluid flow, solute transport and heat transfer continuity equations for 2-D discrete fractures are written as (Therrien & Sudicky, 1996; Holzbecher, 1998):

$$\frac{\partial}{\partial t}\{\rho^{fr}\} = -\nabla \bullet \{\rho^{fr}\mathbf{v}^{fr}\} \pm \Gamma_{mass} + q_{n|I^+} + q_{n|I^-} \quad (4)$$

$$\frac{\partial}{\partial t}\{C^{fr}\} = -\nabla \bullet \mathbf{J}_{solute}^{fr} \pm \Gamma_{solute} + \Omega_{n|I^+} + \Omega_{n|I^-} \quad (5)$$

$$\frac{\partial}{\partial t}\{(\rho\tilde{c})_l T^{fr}\} = -\nabla \bullet \mathbf{J}_{heat}^{fr} \pm \Gamma_{heat} + \Lambda_{n|I^+} + \Lambda_{n|I^-} \quad (6)$$

where the last two terms in each equation denote normal components of fluid flux, solute mass flux and heat exchange across the fracture–matrix interfaces I^+ and I^- .

For variable-density flow conditions, the fluid flux, $q_i = \phi v_i$ [L T^{-1}], is a function of both the freshwater head, h_0 [L], and the fluid relative density, $\rho_r = (\rho/\rho_0) - 1$ [M L^{-3}]. Fluid flux for the matrix and fractures is given by (Bear, 1988):

$$q_i = -K_{ij}^0 \frac{\mu_0}{\mu} \left(\frac{\partial h_0}{\partial x_j} + \rho_r \eta_j \right) \quad i, j = 1, 2, 3 \quad (7)$$

$$q_i^{fr} = -K_0^{fr} \frac{\mu_0}{\mu^{fr}} \left(\frac{\partial h_0^{fr}}{\partial x_j} + \rho_r^{fr} \eta_j \cos \varphi \right) \quad i, j = 1, 2 \quad (8)$$

where φ [–] is the incline of the fracture, with $\varphi = 0^\circ$ for a vertical fracture and $\varphi = 90^\circ$ for a horizontal fracture. The freshwater hydraulic conductivities, K_{ij}^0 and K_0^{fr} [$L T^{-1}$], of both media are given by (Bear, 1988):

$$K_{ij}^0 = \frac{\kappa_{ij} \rho_0 g}{\mu_0} \quad (9)$$

$$K_0^{fr} = \frac{(2b)^2 \rho_0 g}{12 \mu_0} \quad (10)$$

where κ_{ij} [L^2] is the permeability of the porous medium, ρ_0 [$M L^{-3}$] and μ_0 [$M L^{-1} T^{-1}$] are reference values of density and viscosity, respectively, g [$L T^{-2}$] is gravitational acceleration and $(2b)$ [L] is the fracture aperture. Both the fluid density and viscosity are calculated as functions of salinity and temperature (Holzbecher, 1998) over a wide range of salinity and for a temperature range between $0^\circ C$ and $300^\circ C$.

The flow equation is discretized in space by means of a control volume finite element approach, ensuring mass conservation at the elemental and global level. The transport and heat transfer equations are solved using a Galerkin finite element approach. An implicit finite difference scheme is used to discretize the time derivative. Two-dimensional fracture elements and 3-D matrix elements share common nodes in the 3-D grid. Thus, heads, concentrations and temperatures are assumed identical along the fracture-matrix interface. The flow equation is coupled with both the transport and the heat transfer equations. The system of equations is solved by Picard iteration.

Model verification

Variable-density flow in porous media has been verified in 2-D using the Elder (1967) problem of free convection. In 3-D, the model was verified with the salt pool problem, where the impact of freshwater recharge to the stable layering of saltwater below freshwater was investigated experimentally (Oswald & Kinzelbach, 2004). Simulation results presented by Shikaze *et al.* (1998) were used to test density-driven flow in fractured media. Heat transfer in fractured porous media is verified by comparing the model with an analytical solution similar to that presented by Tang *et al.* (1981).

ILLUSTRATIVE EXAMPLES

Vertical brine migration in fractured porous media

For this example, dense plume migration is simulated in two different, yet statistically equivalent fractured networks located in a porous matrix (Fig. 2). Simulations are for a vertical slice of unit thickness and having dimensions 12×10 m. The slice is

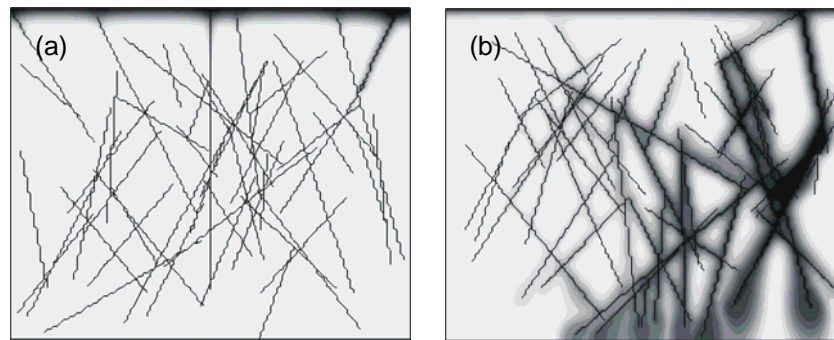


Fig. 2 Simulated concentration at 2 years for 2 different fracture networks. Darker colours correspond to high concentration and lighter colours to low concentration.

discretized with 12 000 square elements of size $\Delta x = \Delta z = 0.1$ m, with local refinement near some fractures. The matrix and fracture properties are identical to those used by Shikaze *et al.* (1998), except that the fracture aperture varies exponentially between 150 and 250 μm . The left and right sides are no-flow boundaries and the bottom and top boundaries are assigned a constant head, $h_0 = 0$, to eliminate forced convection. Similar to Shikaze *et al.* (1998), the top of the domain is assumed to be a salt lake with a constant concentration. All other boundaries are assigned zero dispersive flux for transport. All simulations cover a time of three years and a constant time step size of one month is used. Heat transfer is not considered in this first example.

Simulations show that, for statistically equivalent systems, a different behaviour is observed, depending on the spatial location of fractures representing high-permeability zones. Results range from virtually stable in Fig. 2(a) to completely unstable in Fig. 2(b). The formation of instabilities is restricted to the highly permeable fracture zones. Thus, the fracture network dictates the value of the perturbation wavelength λ , which is the ratio between the domain length (here 12 m) and the number of fingers. The number of fingers in the two cases is 4 and 1, respectively, leading to wavelengths of 3 and 12 m, respectively. Clearly, shorter wavelengths are more stable, whereas systems with long wavelengths are unstable. This observation is consistent with the findings of Simmons *et al.* (2001) who examined variable-density transport in statistically equivalent heterogeneous porous media.

The model was next applied to assess the impact of parameter uncertainties on plume transport. Eight sets of simulations were carried out where individual physico chemical properties were modified. The fracture network chosen is similar to the one depicted in Fig. 2, which allows one to examine the behaviour of the network as a whole instead of that of the few fractures that dominate the system as shown in Fig. 2(b).

Results are not shown here but the sensitivity analysis indicates that increased matrix permeability destabilizes the system because of higher Darcy fluxes in the matrix. The impact of matrix porosity changes on variable-density solute transport was found to be similar to the case where the fluid density is constant. This latter sensitivity has been investigated by Sudicky & McLaren (1992), who have shown that in discretely-fractured porous formations the bulk travel distance is inversely proportional to the porosity. Because fluid fluxes depend on the cube of the fracture aperture, uncertainties in aperture size have a major impact on the results, with large apertures

promoting instability. Finally, a high diffusion coefficient leads to a high matrix diffusion and, therefore, to a drop of concentration within the fractures. Hence, due to the loss of tracer into the matrix, the fractures are depleted in solutes resulting in less buoyancy within the fractures.

Horizontal thermohaline brine migration

Using the physical setup of Schincariol *et al.* (1994), two simulations of the migration of a dense plume have been conducted, for both non-fractured and fractured porous media (Fig. 3). Density contrasts are caused by the solute concentration as well as the fluid temperature. The porous matrix has properties identical to those used by Schincariol *et al.* (1994) and a uniform fracture aperture equal to $40\ \mu\text{m}$ is assumed. A vertical slice of unit thickness, with dimensions $1 \times 0.25\ \text{m}$, is discretized with 40 300 rectangular elements. The element size is smaller at the left boundary ($\Delta x = 1.0\ \text{mm}$, $\Delta z = 2.5\ \text{mm}$), and it increases towards the right ($\Delta x = 2.5\ \text{mm}$, $\Delta z = 2.5\ \text{m}$). A constant horizontal flux is assumed and a solute source is located along a fraction of the left boundary, with a constant concentration of $500\ \text{mg L}^{-1}$. The source also corresponds to a prescribed temperature boundary condition ($T = 244^\circ\text{C}$). Initially, the entire system is solute-free and the uniform initial temperature is 239°C , lower than that at the source. The simulations cover a time of 3 days with time steps gradually increasing from 1 minute to 2 hours. Thermal deformations of the rock are not considered.

The inflowing hot saline fluid has a density lower than the reference density. In this case, the relative density, ρ_r , is negative, resulting in a positive buoyancy effect that can be seen near the source. However, further away from the source, the influence of the solutes on density dominates because advective solute transport is more efficient than conductive heat transfer. Therefore, the fluid density exceeds its reference value and the density contrast, ρ_r , is positive, which results in a noticeable sinking of the fluid.

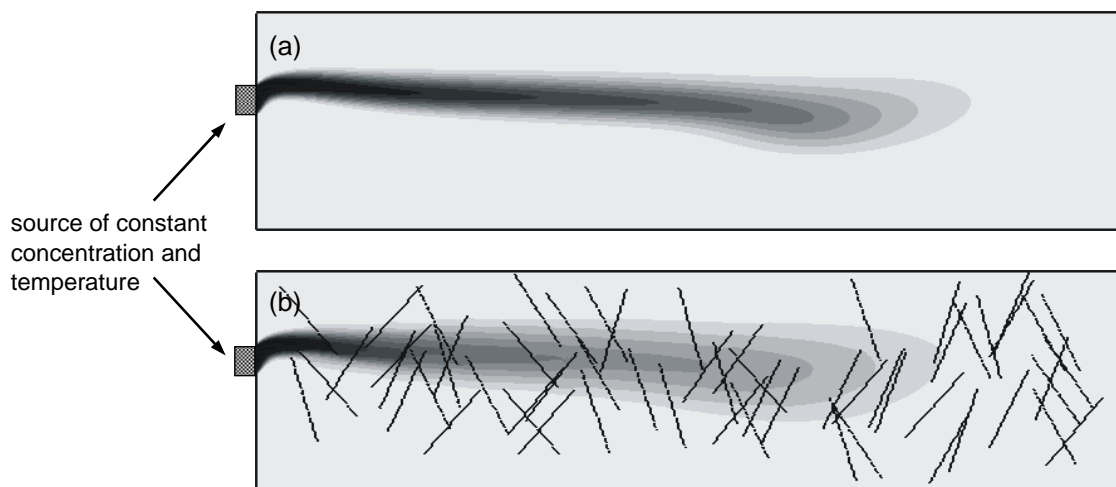


Fig. 3 Migration of a dense plume in porous (a) and fractured porous (b) media.

A second simulation assumes the presence of fractures oriented transversely to the ambient flow direction. The fractures appear to increase the transverse dispersion of the plume. This results in a larger vertical extension of the plume and reduced lateral migration, Fig. 3(b). However, the density contrast, ρ_r , is generally small in these simulations. Therefore, the buoyancy effect in equation (8) is minor and the fractures do not act like preferential pathways as is the case in the previous example.

CONCLUSIONS

The new model has a unique formulation because it enables the simulation of plume migration in realistic fracture networks, as illustrated in the first example. In addition, it is the first model that couples heat transfer and solute transport with variable-density flow in fractured porous media, as illustrated in the second example.

Simulations show that the migration of a dense plume in an irregular fracture network is highly sensitive to the network used. A sensitivity analysis indicates that the system tends to be unstable for large matrix permeability, low matrix porosity, large fracture apertures and low molecular diffusion. Horizontal thermohaline plume transport is controlled by the temperature distribution in the near field and by the solute concentration in the far field. Fractures contribute to the transverse dispersion of the plume.

Acknowledgements We thank the Canadian Water Network (CWN) and the Natural Sciences and Engineering Research Council of Canada (NSERC) for financial support. Author T. Graf thanks the International Council for Canadian Studies (ICCS) and the German Academic Exchange Service (DAAD) for providing a Postgraduate Scholarship stipend.

REFERENCES

- Bear, J. (1988) *Dynamics of Fluids in Porous Media*. Elsevier, New York, USA.
- Elder, J. W. (1967) Transient convection in a porous medium. *J. Fluid Mechanics* **27**(3), 609–623.
- Holzbecher, E. (1998) *Modeling Density-driven Flow in Porous Media*. Springer Verlag, Berlin, Germany.
- Oswald, S. E. & Kinzelbach, W. (2004) Three-dimensional physical benchmark experiments to test variable-density flow models. *J. Hydrol.* **290**(5), 22–42.
- Schincariol, R. A., Schwartz, F. W. & Mendoza, C. A. (1994) On the generation of instabilities in variable density flow. *Water Resour. Res.* **30**(4), 913–927.
- Shikaze, S. G., Sudicky, E. A. & Schwartz, F. W. (1998) Density-dependent solute transport in discretely-fractured geologic media: is prediction possible? *J. Contam. Hydrol.* **34**(10), 273–291.
- Simmons, C. T., Fenstemaker, T. R. & Sharp Jr, J. M. (2001) Variable-density groundwater flow and solute transport in heterogeneous porous media: approaches, resolutions and future challenges. *J. Contam. Hydrol.* **52**(11), 245–275.
- Sudicky, E. A. & McLaren, R. G. (1992) The Laplace transform Galerkin technique for large-scale simulation of mass transport in discretely-fractured porous formations. *Water Resour. Res.* **28**(2), 499–514.
- Tang, D. H., Frind, E. O. & Sudicky, E. A. (1981) Contaminant transport in fractured porous media: Analytical solution for a single fracture. *Water Resour. Res.* **17**(3), 555–564.
- Therrien, R. & Sudicky, E. A. (1996) Three-dimensional analysis of variably saturated flow and solute transport in discretely-fractured porous media. *J. Contam. Hydrol.* **23**(6), 1–44.